CONTRAST MEDIA & MOLECULAR IMAGING

Received: 2 September 2014, Revised: 13 April 2015, Accepted: 20 May 2015, Published online in Wiley Online Library: 11 August 2015

(wileyonlinelibrary.com) DOI: 10.1002/cmmi.1653

Connexin 43-targeted T_1 contrast agent for MRI diagnosis of glioma

Tatiana Abakumova[a], Maxim Abakumov[b], Sergey Shein[a], Pavel Chelushkin[c], Dmitry Bychkov[d], Vladimir Mukhin[b], Gaukhar Yusubalieva[a], Nadezhda Grinenko[a], Alexander Kabanov[e,f], Natalia Nukolova[a,e]* and Vladimir Chekhonin[a,b]

Glioblastoma multiforme is the most aggressive form of brain tumor. Early and accurate diagnosis of glioma and its borders is an important step for its successful treatment. One of the promising targets for selective visualization of glioma and its margins is connexin 43 (Cx43), which is highly expressed in reactive astrocytes and migrating glioma cells. The purpose of this study was to synthesize a Gd-based contrast agent conjugated with specific antibodies to Cx43 for efficient visualization of glioma C6 *in vivo*. We have prepared stable nontoxic conjugates of monoclonal antibody to Cx43 and polylysine–DTPA ligands complexed with Gd(III), which are characterized by higher T_1 relaxivity (6.5 mM^{-1} s^{-1} at 7 T) than the commercial agent Magnevist® (3.4 mM^{-1} s^{-1}). Cellular uptake of Cx43-specific T_1 contrast agent in glioma C6 cells was more than four times higher than the nonspecific IgG-contrast agent, as detected by flow cytometry and confocal analysis. MRI experiments showed that the obtained agents could markedly enhance visualization of glioma C6 *in vivo* after their intravenous administration. Significant accumulation of Cx43-targeted contrast agents in glioma and the peritumoral zone led not only to enhanced contrast but also to improved detection of the tumor periphery. Fluorescence imaging confirmed notable accumulation of Cx43-specific conjugates in the peritumoral zone compared with nonspecific IgG conjugates at 24 h after intravenous injection. All these features of Cx43-targeted contrast agents might be useful for more precise diagnosis of glioma and its borders by MRI. Copyright © 2015 John Wiley & Sons, Ltd.
Additional supporting information may be found in the online version of this article at the publisher's web site.

Keywords: T_1 contrast agent; cellular targeting; MRI; targeted imaging; connexin 43; glioma

1. INTRODUCTION

About 1.5 million people in the USA are diagnosed with cancer every year, and 30% of them have a brain tumor (1,2). Glioblastoma multiforme is one of the most common and aggressive forms of brain tumor, and has an extremely poor prognosis: median survival time of patients is less than 14 months (1). The crucial point of successful treatment and prolongation of patient lifespan is an early diagnosis of glioma and its borders. Contrast agents for magnetic resonance imaging (MRI) containing paramagnetic ions such as gadolinium are often used to improve the contrast between tissues, thereby providing more accurate diagnosis of a desirable region (3). Low molecular weight contrast agents (Magnevist®, Gadovist®, Omniscan®) cannot easily penetrate an intact blood–brain barrier (BBB) (4), although they are able to accumulate in the brain with disrupted BBB and visualize its pathologies by T_1-weighted MRI (5). However, these contrast agents are rapidly eliminated from the blood pool due to their low molecular weight. Moreover, they can extravasate from the vasculature into surrounding tissues, leading to poor contrast of a tumor compared with healthy tissues.

To increase circulation time of contrast agents and their accumulation in a tumor due to the enhanced permeability and retention (EPR) effect (6), these agents can be conjugated with various macromolecules such as proteins, dextrans and polyamino acids (7). For example, a conjugate of poly-L-lysine with DTPA-Gd chelates (PLL–DTPA-Gd) was used for tumor

* *Correspondence to: N. Nukolova, Department of Fundamental and Applied Neurobiology, Serbsky National Research Center for Social and Forensic Psychiatry, Moscow, Russia. E-mail: nukolova@serbsky.ru*

a *T. Abakumova, S. Shein, G. Yusubalieva, N. Grinenko, N. Nukolova, V. Chekhonin*
Department of Fundamental and Applied Neurobiology, Serbsky National Research Center for Social and Forensic Psychiatry, Moscow, Russia

b *M. Abakumov, V. Mukhin, V. Chekhonin*
Department of Medical Nanobiotechnology, Pirogov Russian National Research Medical University, Moscow, Russia

c *P. Chelushkin*
Laboratory of Synthesis of Peptides and Polymer Microspheres, Institute of Macromolecular Compounds, Russian Academy of Sciences, St Petersburg, Russia

d *D. Bychkov*
Department of Geology, Lomonosov Moscow State University, Moscow, Russia

e *A. Kabanov, N. Nukolova*
Department of Chemistry, Laboratory Chemical Design of Bionanomaterials, Lomonosov Moscow State University, Moscow, Russia

f *A. Kabanov*
Center for Nanotechnology in Drug Delivery and Division of Molecular Therapeutics, UNC Eshelman School of Pharmacy, University of North Carolina at Chapel Hill, Chapel Hill, NC, USA

diagnosis of mammary adenocarcinoma (8) and glioma in rodent models (9). Moreover, PLL–DTPA-Gd is in the preclinical stage for angiography (Bayer, Leverkusen, Germany).

Further improvement of MRI diagnosis of brain tumor and its periphery is possible due to active targeting. Specific targeting groups conjugated with contrast agents can improve recognition and accumulation within the particular tissue. For example, the enhancement of glioma visualization was observed for paramagnetic liposomes coupled with monoclonal antibodies (mAb) to endoglin (CD105), the key protein in tumor angiogenesis (10). Lysine-based dendritic macromolecules modified with chlorotoxin also improved visualization of glioma (11). Compared with conventional contrast agents, these approaches allowed enhancement of the visualization of brain tumors. However, one of the most important tasks – detection of glioma borders – still remains insufficiently addressed.

Connexin 43 (Cx43) is an integral membrane protein, which plays a key role in cell–cell communication. It is highly expressed in reactive astrocytes, migrating glioma cells and brain endothelial gap junctions (12,13). The level of Cx43 expression is associated with active invasion and migration activity of glioma cells, and has been intensively studied (14,15). Overexpression of Cx43 was observed in the migrating cells in the peritumoral zone of glioma C6 (16). Thus, the targeted delivery of contrast agent to Cx43-positive cells might improve the visualization of glioma, especially its peritumoral zone. The conjugation of macromolecular contrast agents with targeting groups such as monoclonal antibodies to Cx43 can be a promising approach for development of Cx43-targeted contrast agent. The purpose of this study was to synthesize the Cx43-targeted contrast agent, mAbCx43-PLL–DTPA-Gd, and evaluate its potential for MRI visualization of glioma and its borders.

2. RESULTS

2.1. Synthesis and analysis of targeted contrast agent

We synthesized the Cx43-targeted contrast agents in two steps (Fig. S1): (1) preparation of PLL–DTPA conjugates with different amounts of DTPA ([DTPA]:[Lys] ratio was 1:10 and 1:1) and (2) their conjugation with monoclonal antibodies to Cx43 (mAbCx43) (molar ratio [mAb]:[PLL–DTPA] was 1:5 or 1:10). The resulting mAbCx43-PLL–DTPA conjugates were complexed with $GdCl_3$ and purified by gel filtration chromatography (Sepharose CL-6B, HEPES).

ELISA analysis of the obtained contrast agents modified by different amounts of PLL revealed that mAbCx43-PLL–DTPA-Gd specific contrast agent bound to its target molecule (retained activity was about 85%), while IgG-PLL–DTPA-Gd had no or little nonspecific binding (about 5%) (Fig. S2). Interestingly, when $mPEG_{5K}$-PLL_{50} was used instead of PLL_{100}, the final conjugate was not able to bind to its target molecule, as detected by ELISA (retained activity was less than 10%). Most probably, this was the result of the steric shielding of the binding site of the mAb by PEGylated polymer (17). The difference in the amount of DTPA attached to PLL (ratio 1:10 or 1:1) influenced the complexation of Gd(III) to the final products: 50 versus 500 μg Gd(III) per mg of mAb, as detected by XRF. Amino acid analysis revealed that the number of PLL chains per mAb was 11 ± 2 and 13 ± 3 for conjugates with [DTPA]:[Lys] ratios of 1:10 and 1:1, respectively (Table S1). To increase the number of chelating groups per mAb, we synthesized the targeted contrast agent using the following molar ratios: [mAb]:[PLL–DTPA] = 1:10 and [DTPA]:[Lys] = 1:1. In this case we were able to attach about 65 ± 3 DTPA molecules per PLL chain, as detected by ^{1}H-NMR (Fig. S3), and complex this conjugate with 40 ± 5 Gd(III) ions per PLL–DTPA molecule, as detected by XRF. The DTPA loading by Gd(III) was 52 ± 8 mol.%. The total Gd(III) loading was about 520 ions per mAb and the molecular weight of the targeted contrast agent was about 850 kDa. Finally, the T_1 relaxivity of mAbCx43-PLL–DTPA-Gd contrast agent was 6.5 ± 0.5 mM^{-1} s^{-1} per Gd at 7 T (17 °C, HEPES), whereas these values for the commercially available analog Magnevist® and PLL–DTPA-Gd were 3.4 ± 0.4 and 4.4 ± 0.6 mM^{-1} s^{-1} per Gd, respectively.

The obtained mAbCx43-PLL–DTPA-Gd contrast agents did not form either aggregates or precipitates in HEPES buffer or in blood serum (10% v/v). The protein concentration in the solution did not change after centrifugation, as demonstrated by BCA assay, indicating the high dispersion stability of the samples. Moreover, these agents retained their immunochemical activity after storage in HEPES (−20 °C for three weeks or 4 °C for one week), as detected by ELISA (Fig. S2(c)).

2.2. *In vitro* cytotoxicity of targeted contrast agents

We analyzed the cytotoxicity of targeted contrast agents by an MTS test on glioma C6 and HEK293 cell lines (Fig. 1(a)). The contrast agent, modified with DTPA in the ratio [DTPA]:[Lys] = 1:10, had a cytotoxic effect on both cell lines. IC_{50} values were 1.58 μg Gd/mL and 1.88 μg Gd/mL for HEK293 and glioma C6, respectively. On the other hand, the contrast agent with a higher amount of DTPA (ratio 1:1) did not exhibit cytotoxicity up to 0.6 mg Gd/mL (Fig. 1(a)). Decrease in cytotoxicity was not unexpected, since positively charged amino groups of PLL may cause a toxic effect (18). The higher degree of their conversion into noncharged amide groups led to lower cytotoxicity. For concentrations up to 2 mg/mL, no cytotoxicity was found with Magnevist®. The contrast agent with the molar ratio [DTPA]:[Lys] = 1:1 possessed noticeably lower toxicity; therefore, we proceeded with all subsequent experiments using this type of contrast agent.

2.3. Cellular uptake of targeted contrast agents

We used confocal microscopy to study the ability of specific mAbCx43-PLL–DTPA-Gd, nonspecific IgG-PLL–DTPA-Gd and nontargeted PLL–DTPA-Gd to bind the antigen in glioma C6 cells, which are known for overexpression of Cx43 antigen (16). We used Alexa 488-labeled secondary antibodies to show the increased accumulation of targeted contrast agents in cells compared with nonspecific IgG-contrast agent or PLL–DTPA-Gd (Fig. 2(a)). Moreover, we performed immunofluorescent analysis with double staining using Alexa 594 secondary antibodies to confirm the stability of the obtained conjugates in the cells (Fig. 2(b)). Double staining showed that the contrast unit (fluorescein-labeled PLL–DTPA-Gd; green color in Fig. 2(b)) had the same location in the live glioma cell as antibodies (red color in Fig. 2(b)), indicating that the conjugate bound to the cells as an entire construction without any dissociation or cleavage.

Cellular uptake of the contrast agent was time and concentration dependent in glioma C6 cells, as determined by flow cytometry (Fig. 3). The uptake of the specific contrast agent was four times higher than for the nonspecific agent after incubation for 30 min. As expected, the difference between them reduced (from four- to twofold) with increasing concentration (from 1 to 5 μM) (Fig. 3(a)). Moreover, the distinction in accumulation decreased

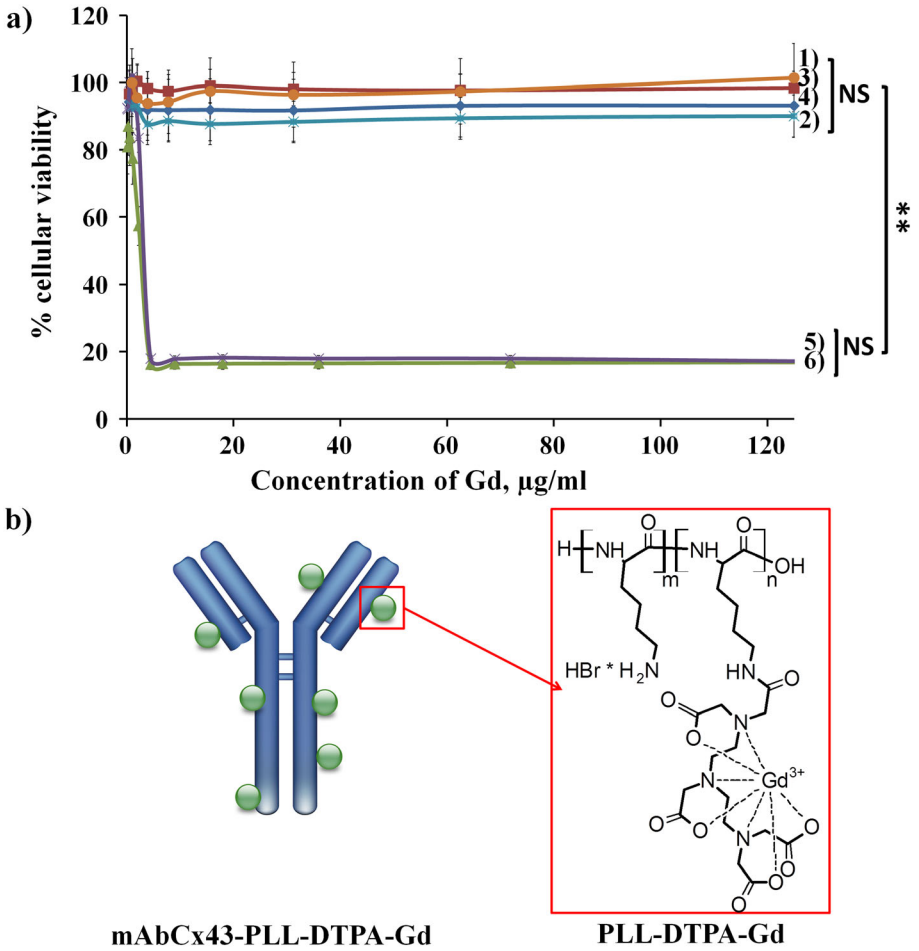

Figure 1. a) In vitro cytotoxicity of the targeted T_1-contrast agents (mAbCx43-PLL-DTPA-Gd) in glioma C6 and HEK293 cell lines. Cytotoxicty of Magnevist® in (1) C6 and (2) HEK293 cells and contrast agents with [DTPA]:[Lys] ratio = 1:1 in (3) C6 and (4) HEK293 cells; contrast agents with [DTPA]:[Lys] ratio = 1:10 in (5) C6 and (6) HEK293 cells. Data are mean ± SEM (n=4, ** - $p<0.01$, NS - not significant. b) Structure of the Cx43-targeted contrast agent (mAbCx43-PLL-DTPA-Gd).

with prolongation of incubation time: after 1 h of exposure the difference between uptake of specific and nonspecific agents was about 20%, indicating saturation of C6 cells (Fig. 3(b)).

2.4. *In vivo* MR imaging

For MRI evaluation all contrast agents (Cx43-specific and nonspecific contrast agents, and Magnevist®) were i.v. injected into rats bearing glioma C6 at the same dose (0.05 mmol Gd/kg). We measured contrast-to-noise ratio (CNR) for quantitative assessment of enhancement and efficacy of the contrast agents. At the earlier time points (up to 1 h after injection) there were no significant differences in accumulation between Cx43-targeted contrast agent and all controls (Fig. 4(a)). All groups showed about 1.5-fold enhancement compared with the initial signal intensity. CNR values for the Cx43-targeted agent gradually increased with time, indicating better contrast enhancement in the tumor tissue. We detected the maximum difference in CNR values for the targeted agent and controls (more than twofold) 24 h after injection (Fig. 4(a)). Interestingly, there was a sharp decrease in CNR values for the nonspecific IgG-conjugate 1 h after injection, while in the case of Magnevist® there was a slow reduction.

The MRI measurements of tumor area allow detection of glioma borders for future surgical resection. The visualized tumor area was significantly expanded in the case of Cx43-specific contrast agents (175% of initial visualized area) (Fig. 4(b)) compared with Magnevist® and nonspecific contrast agents (120% and 95% of initial visualized area, respectively) at 24 h after injection. Interestingly, in the first 4 h there was no significant difference in visualized tumor area between Cx43-specific agent and Magnevist® – both of them improved visualization of glioma borders by 30% – while IgG contrast agent did not change the visualized glioma area during the studied period (about 95% from initial visualized area) (Fig. 4(b)).

2.5. *In vivo* accumulation of targeted contrast agents

To prove that the enhanced accumulation of the Cx43-targeted contrast agent in glioma was due to specific binding, we analyzed distribution of fluorescent-labeled agents in the brain 24 h after a single i.v. injection. We evaluated average fluorescence of Cx43-specific and nonspecific contrast agents, as well as PLL–DTPA, in a whole brain using an IVIS Spectrum CT (Perkin Elmer). The average fluorescence of Cx43-targeted contrast agent was five times higher than that for PLL–DTPA and about three times higher than that for nonspecific IgG-agent (Fig. 5(a)). Comparative analysis of brain sections performed using fluorescent microscopy (DMI 6000, Leica) revealed substantial distinction in

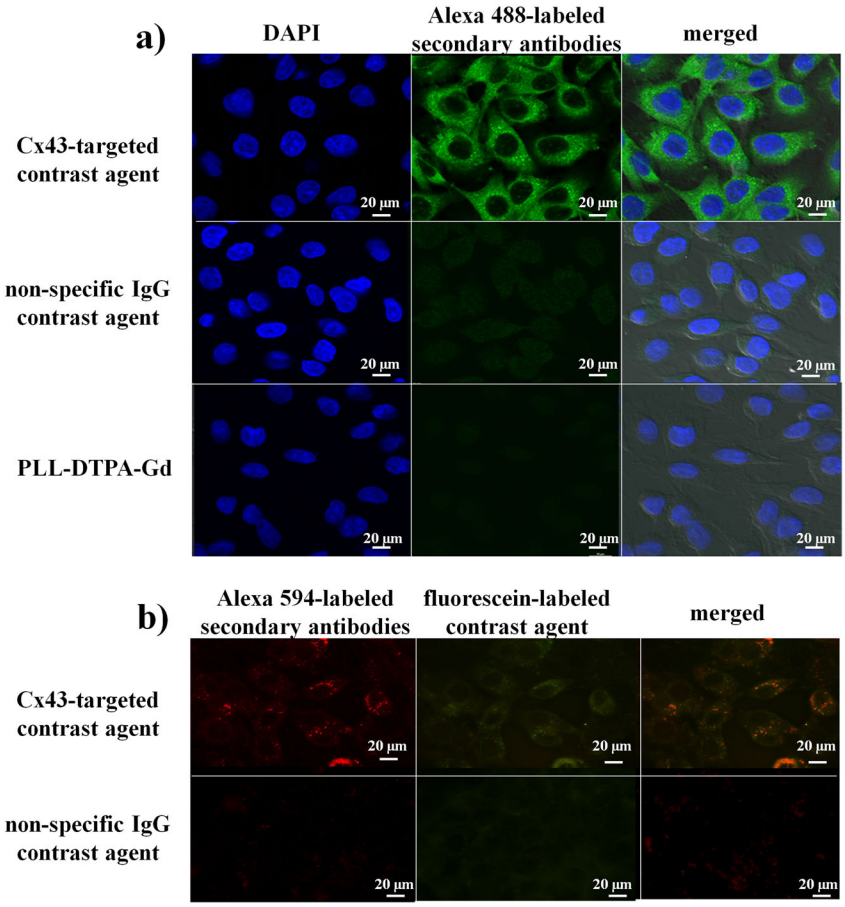

Figure 2. Confocal microscopy of the targeted contrast agent on a) fixed and b) live glioma C6 cells. Fixed cells were incubated for 1 h with contrast agents (Cx43-specific and non-specific IgG-contrast agents, PLL-DTPA-Gd), followed by staining with Alexa 488-labeled secondary antibodies (green). Live cells were exposed to fluorescein-labeled mAb-PLL-DTPA-Gd and IgG-PLL-DTPA-Gd (green) contrast agents for 45 min, followed by staining with Alexa 594-labeled secondary antibodies (red). Nuclei were strained with DAPI (blue).

the distribution of the studied contrast agents. Fig. 5(b) shows intensive accumulation of Cx43-targeted agent in the tumor and predominately in the peritumoral zone, where Cx43 is mainly expressed (16). This pattern was not observed for PLL–DTPA or IgG-contrast agents.

It should be noted that, if glioma C6 consisted of extracranial and intracranial parts, we detected a vast accumulation of the contrast agent in the extracranial part (Fig. S4). For example, the difference in fluorescence intensity between extracranial and intracranial gliomas was about 25-fold for Cx43-specific agent and sevenfold for the nonspecific agent. In the case of similar fluorescence intensities in the intracranial portion, the accumulation in the extracranial part was three times higher for Cx43-targeted agent (Fig. S4(b)).

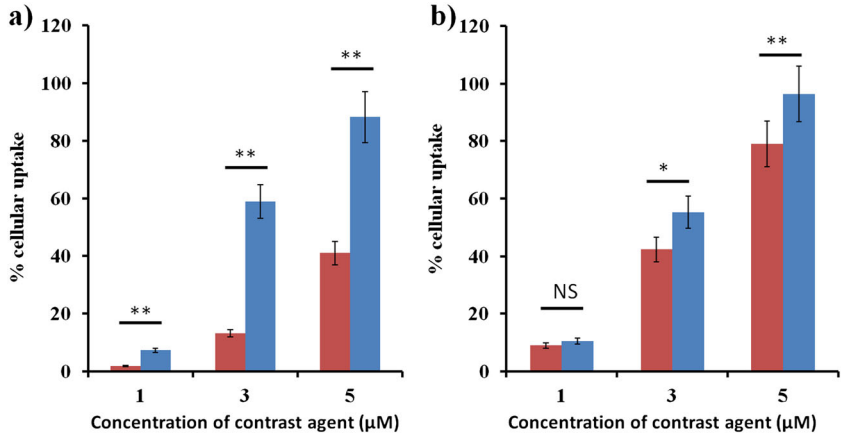

Figure 3. Cellular uptake of specific (blue) and non-specific (red) T_1-contrast agents in glioma C6 cells after incubation for a) 30 min or b) 1 h. Data are mean ± SEM (n = 3), *- $p < 0.05$, **- $p < 0.01$, NS - not significant.

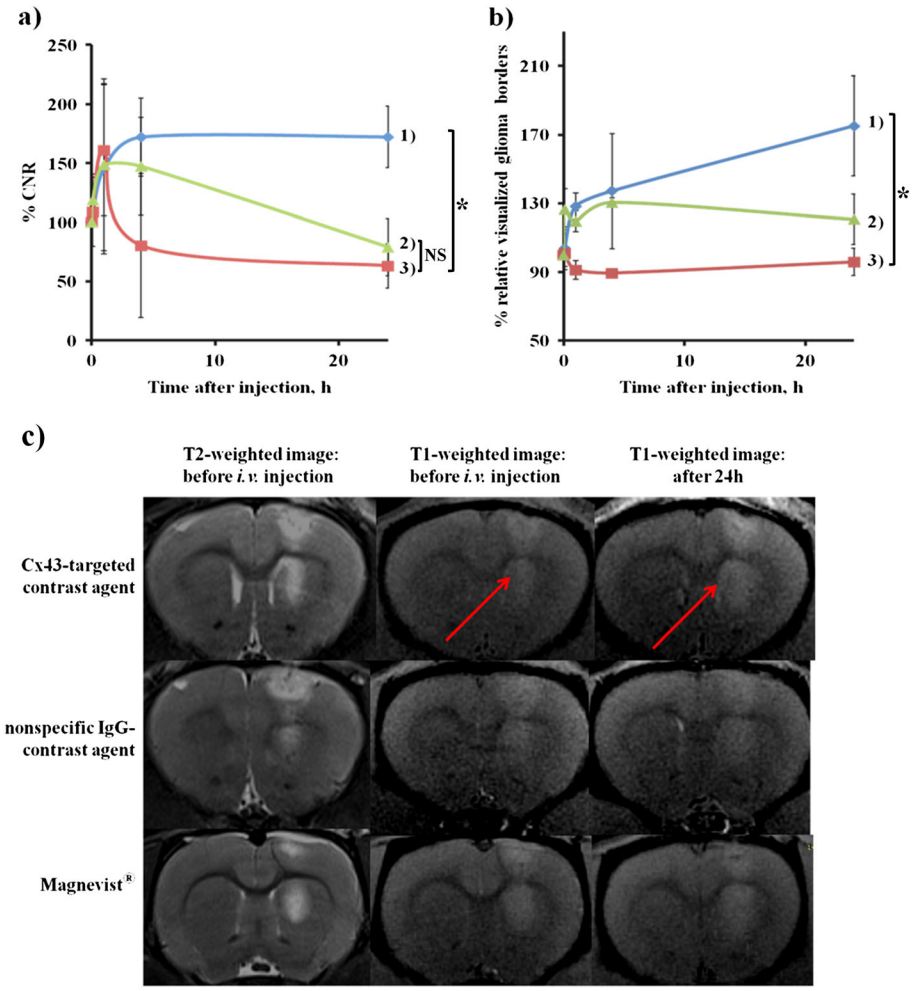

Figure 4. In vivo MRI analysis of contrast agents in rats bearing glioma C6. Plot of dynamic changes of a) contrast-to-noise ratio and b) relative visualized glioma area after i.v. injection of (1) Cx43-specific contrast agent, (2) Magnevist® and (3) non-specific IgG-contrast agent. c) T_1-weighted images of glioma C6 before and at 24 h after i.v. injection of contrast agents. T_2-weighted images of glioma C6 at 14th day after implantation. Data are mean ± SEM (n = 4). Statistical significance at 24 h: *- $p<0.05$, NS - not significant.

Moreover, the preliminary data on the distribution of the contrast agents in rats indicated that obtained agents were excreted mainly through the kidneys without considerable accumulation in the liver, spleen or lungs, as detected by IVIS and MRI analysis (Fig. S5). MRI analysis of the body suggested that the majority of agents were eliminated within 24 h (Fig. S5(a)). Probably this occurred due to the dissociation of the agent *in vivo* (namely, detachment of the DTPA–PLL chains from the antibody). However, the proper studies should be conducted to draw a conclusion on the biodistribution and stability of this agent *in vivo*.

3. DISCUSSION

Detection of the brain tumor and its borders at the early stage is a milestone in the improvement of the quality of life and life expectancy of patients. This challenging task could be successfully addressed using MRI with contrast agents targeted to the specific molecular markers of the disease (19,20). To enhance the local concentration of contrast agents in the tumor and increase the sensitivity of MRI, we developed the macromolecular Gd-based Cx43-targeted contrast agent. Connexin 43 is an integral membrane protein, which is overexpressed in mobilized glioma cells of the peritumoral space and reactive astrocytes (13,21). Therefore, it appears to be an attractive target for diagnosis of the brain tumor and the peritumoral zone (22). Macromolecular contrast agents (e.g. blood pool or intravascular contrast agents) could expand the imaging window from 1 min to 1 h due to their high molecular weight (23). Moreover, they have higher T_1 relaxivity than Magnevist® and other low molecular weight complexes (3). Thus, the combination of the properties of macromolecular agents and benefits from the active targeting of glioma cells could lead to a synergistic increase in efficiency of glioma visualization *in vivo* and decrease the effective dose (<0.1 mmol Gd/kg). Here we propose the preparation of T_1 contrast agent based on a specific mAb to Cx43 and chelate complexes of Gd(III) for visualization of glioma and the peritumoral zone *in vivo*.

To achieve the maximum concentration of contrast agent in the tumor site after injection, we conjugated the targeting group (mAb to Cx43) with multiple PLL–DTPA chains. We prepared the targeted contrast agent mAbCx43-PLL–DTPA-Gd (molar ratios [mAb]:[PLL–DTPA] = 1:10 and [DTPA]:[Lys] = 1:1) under mild conditions and thoroughly purified it via additional complexation of Gd(III) with EDTA. It is known that free Gd(III) ions are very toxic due to their interference with calcium channels and protein

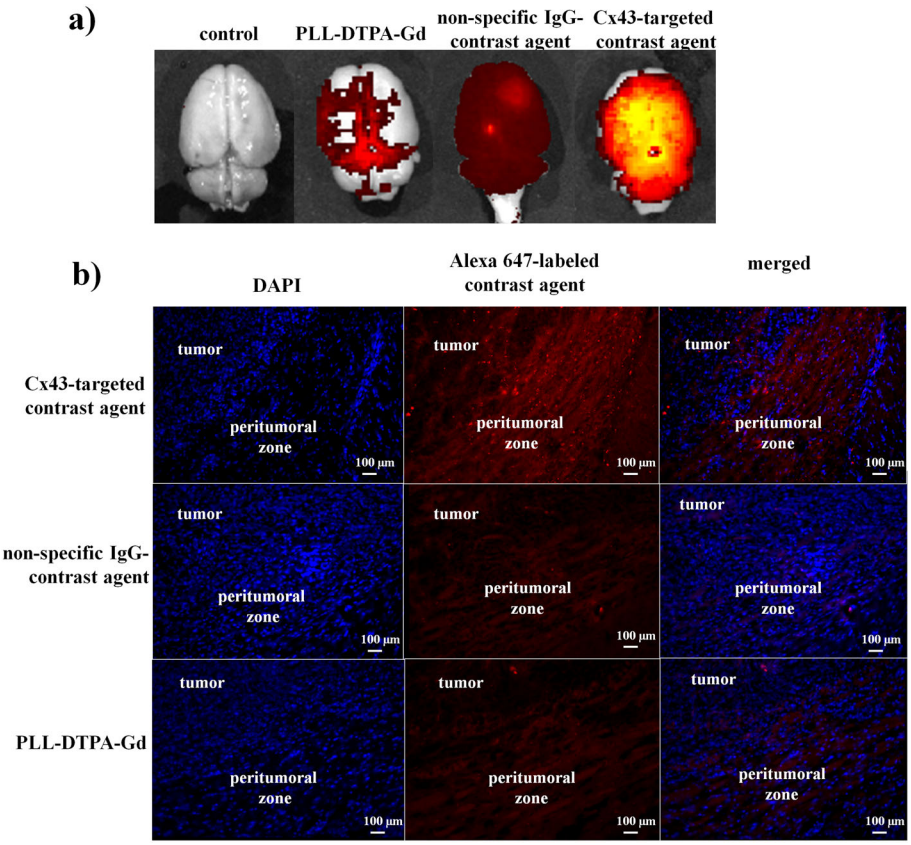

Figure 5. Fluorescent analysis of brains of rats injected with Alexa 647-labeled contrast agents at 24 h after i.v. injection. a) Radiant efficiency of fluorescence in the brains, following injection of PLL-DTPA, non-specific IgG-contrast, and Cx43-specific contrast agents (control - saline); b) fluorescent analysis of the brain sections of rats injected with Cx43-specific and non-specific IgG-contrast agents (red). Brain sections were stained with DAPI (blue).

binding sites (24,25). The obtained targeted contrast agents remained stable and retained their immunochemical activity during storage. The relaxivity values were about twice as high as for the clinically approved agent Magnevist® (26,27). This could be due to slower rotational dynamics of macromolecules (28–30) and second-sphere effects (31). The cellular uptake of mAbCx43-PLL–DTPA-Gd was about four times higher than that of IgG-PLL–DTPA-Gd in Cx43-overexpressing cells, as detected by flow cytometry. These results confirmed that the Cx43-specific targeted contrast agents were able to recognize their molecular sites and selectively accumulate in glioma cells.

MRI experiments on obtained Cx43-targeted contrast agents revealed their efficacy in the glioma model. Analysis of CNR allowed us to quantify the contrast enhancement of the tumor site compared with normal tissue and noise. Cx43-targeted contrast agent improved visualization of glioma even at 24 h after injection due to its significant accumulation in the tumor region. Meanwhile, tumor enhancement did not persist at 24 h post administration of the nonspecific contrast agent or Magnevist®. High accumulation and retention of mAbCx43-PLL–DTPA-Gd in glioma can be explained by the synergistic effect of two mechanisms: passive targeting via long circulation time and active targeting via specific binding of contrast agent to Cx43-positive cells in the tumor. Gradual decreasing of tumor visualization by Magnevist® was probably due to its rapid elimination from the blood pool and nonspecific extravasation into surrounding tissues (32). In the case of the IgG-modified agent the decrease of contrast might be due to its rapid clearance by the reticuloendothelial system (33). In contrast to the above controls, the Cx43-targeted contrast agent not only retained high CNR values even 24 h post injection, but also improved detection of the borders with time.

These data correlate with the recent studies on glioma-specific contrast agents based on dendrigraft PLL with conjugated chlorotoxin (11). The authors showed a similar trend of glioma visualization using the same dose of contrast agent (0.05 mmol Gd/kg). However, in the present study we could achieve considerably better contrast enhancement at the later time points (172% versus 110% at 24 h). Han *et al*. could not detect considerable contrast enhancement of glioma using targeted Gd-based dendrimers over 24 h (34). The maximum CNR value was 122% for targeted and nontargeted Gd-based dendrimer contrast agents (Gd-DTPA–PAMAM-PEG-T7 and Gd-DTPA–PAMAM-PEG) and 124% for Magnevist® at 5 min post injection. Notably, in the present study we achieved 150% CNR at the same time point. Significant contrast enhancement was demonstrated for Gd-DTPA liposomes targeted to CD105 using a very low injected dose (3 μmol Gd/kg) (35). Unfortunately, comparison of these results is rather questionable since a subcutaneous model of glioma was used, which does not reflect accurately the situation in the brain tumor due to the absence of the BBB. In the present study we have demonstrated the combination of contrast enhancement of glioma with improvement of tumor border detection, which is a very important feature for more exact diagnosis of tumors. Improved ring-like visualization of glioma periphery was also shown by Qiu *et al*. using

endoglin-targeted paramagnetic liposomes (10). However, the injected dose of contrast agent (0.1 mmol Gd/kg) used in the above work was twice as high as that used in the present study (0.05 mmol Gd/kg).

Using fluorescent analysis of the brain slices, we detected the improved accumulation of Cx43-targeted contrast agents in the peritumoral zone compared with all controls 24 h after i.v. injection. In this zone infiltration and migration of glioma cells into the surrounding tissues is observed (36). Intensive invasion of glioma cells provides resistance and rapid progression of brain tumor. After surgical removal of brain tumor, these cells of the peritumoral zone may cause its relapse. Therefore, the possibility of selective diagnosis of tumor borders can significantly increase the efficiency of the treatment.

However, in spite of the advantages of the obtained contrast agent (low cytotoxicity, specific *in vitro* and *in vivo* accumulation, improved tumor border detection) it has a number of limitations. Undoubtedly, for clinical use the contrast of images (CNR values) should be improved. In turn, this may lead to even better detection of tumor borders for more precise diagnosis of glioma by MRI. We believe that it is possible by optimization of the contrast unit in the developed construction (e.g. PEGylated polymers with optimal length and/or topology and complexed Gd(III), use of other chelating units, e.g. DOTA, etc). In addition, it is necessary to analyze biodistribution, systemic toxicity and *in vivo* stability of the obtained agents for better understanding of the behavior of this system in the body and prediction of its safety for further use. Moreover, the successful use of all antibody-based conjugates relies on the expression of antigens in the targeted site, which should be analyzed prior to their use. All these limitations should be taken into account for further development and use of the obtained agents.

In summary, we have shown that the Cx43-targeted contrast agent could efficiently visualize glioma C6 and its borders both *in vitro* and *in vivo*. The presented contrast agent exhibited higher contrast and longer imaging time in the T_1-weighted MRI diagnosis of glioma C6 compared with Magnevist® and nonspecific IgG-contrast agent. Moreover, the Cx43-specific contrast agent could be used at very low dose (0.05 mmol Gd/kg), which is certainly advantageous for its further use.

4. EXPERIMENTAL

4.1. Materials

Gadolinium(III) chloride hexahydrate ($GdCl_3$*$6H_2O$), diethylenetriaminepentaacetic acid (DTPA), polylysine hydrobromide with molecular weight 15–30 kDa (PLL), 1-ethyl-3-(3-dimethylaminopropyl) carbodiimide (EDC), phosphate buffer saline (PBS), tetramethylbenzidine (TMB), 4,6-diamidino-2-phenylindole (DAPI), PD-10 desalting columns, and Sepharose CL-6B were purchased from Aldrich Chemical Co. (St Louis, MO, USA). DMEM medium, fetal bovine serum (FBS), 0.25% trypsin/EDTA, Alexa Fluor 594 and 488-labeled goat anti-mouse IgG were from Life Technologies (Carlsbad, CA, USA). 3-(4,5-dimethylthiazol-2-yl)-5-(3-carboxy-methoxyphenyl)-2-(4-sulfophenyl)-2H-tetrazolium, inner salt (MTS) was purchased from Promega (Fitchburg, WI, USA). The avidin–biotin complex kit (ABC-kit) was from Vector Laboratories (Burlingame, CA, USA). The micro BCA protein assay kit was from Pierce Biotechnology (Waltham, MA, USA). Magnevist® was from Bayer AG (Leverkusen, Germany). Monoclonal antibodies to Cx43 and nonspecific immunoglobulins G (IgG) were obtained as previously described (37).

4.2. Synthesis and analysis of targeted contrast agent

The targeted contrast agent was synthesized by conjugating monoclonal antibody (mAb) with PLL–DTPA adducts and then complexed with Gd(III). First, we synthesized PLL–DTPA adducts with different degrees of DTPA modification ([DTPA]:[Lys] ratio 1:10 and 1:1), purified them using PD-10 desalting columns and lyophilized them. Then, mAbs to Cx43 and nonspecific IgG were activated by EDC:NHS (ratio 1:1) and conjugated with PLL–DTPA at molar ratio 1:10 or 1:5 (HEPES buffer, 4 °C, overnight). Finally, mAb-PLL–DTPA was complexed with $GdCl_3$*$6H_2O$ (0.2 M acetate buffer, pH 5.5, 4 °C, overnight). The twofold excess of EDTA was added for complexation of Gd(III), which is unbound or weakly bound to the obtained product. Then the obtained contrast agents were purified using size exclusion chromatography (Sepharose CL-6B, 0.3 mL/min, HEPES, pH 7.4), sterilized (0.22 μm, Fisherbrand) and stored at 4 °C until further use.

For *in vitro* and *in vivo* experiments we synthesized fluorescent-labeled targeted contrast agents, using fluorescein or Alexa Fluor 647 carboxylic acid, succinimidyl ester (Life Technologies, Carlsbad, MA, USA). We prepared fluorescent-labeled PLL–DTPA adducts, which were conjugated to mAb and complexed with Gd(III) as described above. The Supporting Information contains details of the experimental setup.

The immunochemical activity of the obtained agents (targeted contrast agents, free mAb to Cx43 (positive control) and nonspecific IgG (negative control)) was analyzed by enzyme-linked immunosorbent assay (ELISA). The concentration of Gd(III) was analyzed by the 'dried drop' method using X-ray fluorescence analysis (XRF) ('REspect' XRF spectrometer, Tolokonnikov, Russia) with addition of molybdenum as an inner standard. PLL–DTPA adducts were analyzed by proton nuclear magnetic resonance spectroscopy (^{1}H NMR) using a Bruker Avance 400 (400 MHz, D_2O, pH 7.0, 25 °C). Amino acid analysis was performed on a System 6300 amino acid analyzer (Beckman, Germany).

Dispersion stability of mAb-PLL–DTPA-Gd was visually evaluated in blood serum (10% v/v, 37 °C, overnight, 4 mg/mL) and HEPES buffer (r.t. and 4 °C for one week or −20 °C for three weeks, 4 mg/mL) for precipitation. Moreover, the sedimentation stability of targeted contrast agent was demonstrated by analyzing the protein concentration in the solution before and after its centrifugation (HEPES, 3000 rpm, 10 min) using micro BCA assay. Preservation of the specific affinity of the obtained contrast agents was analyzed by ELISA (HEPES, storage for one week at 4 °C or for three weeks at −20 °C, 4 mg/mL).

4.3. Relaxivity measurement

T_1-relaxivity of the obtained contrast agents and Magnevist® was calculated per Gd as described by Tamura *et al*. (38). A set of images of each sample (concentration 0.1–0.5 mmol Gd(III) in 1 mL HEPES buffer) was obtained using an inversion-recovery sequence with the following parameters: TR = 16 000, TE = 7.1, TI = 50, 100, 200, 400, 600, 800, 1000, 1500, 1980 (17 °C, 7 T, Bruker BioSpin, ClinScan, Ettlingen, Germany). The signal intensity (SI) of each sample at different TI values was measured using ImageJ Software (NIH Image, USA). Curves of SI dependence on TI for each concentration were constructed [38]; and T_1 relaxation time was determined by Mathcad approximation

(Needham, MA, USA). The dependence of reverse T_1 relaxation time on concentration of Gd(III) was plotted, and T_1 relaxivity calculated as the tangent of the inclination angle.

4.4. *In vitro* cytotoxicity

Human embryonic kidney cells (HEK 293) and rat glioma C6 cells were cultured in DMEM supplemented with 10% FBS (37 °C, 5% CO_2). HEK 293 and glioma C6 cells were seeded in 96-well plates (5000 cells/well) in DMEM medium for 48 h before experiments. Then cells were treated with the targeted contrast agents at concentrations up to 0.6 mg Gd/mL and Magnevist® at concentrations up to 2 mg Gd/mL for 24 h, washed, and cultured for an additional 24 h in fresh medium at 37 °C. Cytotoxicity was determined by colorimetric MTS assay. The Supporting Information contains details of the experimental setup.

4.5. Flow cytometry

Glioma C6 cells (10 000 cells/well) were grown in 48-well plates in DMEM medium for 2 days before experiments. Then cells were treated with fluorescein-labeled mAbCx43-PLL–DTPA-Gd and IgG-PLL–DTPA-Gd at different concentrations (1, 3 and 5 μM of contrast agents) for 30 min and 1 h at 37 °C. After incubation, cells were washed twice with PBS, trypsinized (0.25% trypsin/EDTA, 5 min) and fixed with 4% paraformaldehyde. Cells were analyzed using a MACSQuant flow cytometer (Miltenyi Biotec, Teterow, Germany). The percentage of positive cells was calculated using MACSQuantify software (Miltenyi Biotec, Teterow, Germany).

4.6. Confocal microscopy

Glioma C6 cells were fixed with 4% paraformaldehyde (30 min, 4 °C), pre-incubated with 10% goat serum (30 min, r.t.) to block nonspecific binding sites on cell membrane and washed with PBS. Then C6 cells were exposed to mAb-PLL–DTPA-Gd, IgG-PLL–DTPA-Gd and PLL–DTPA-Gd contrast agents (2 μM contrast agent, 1 h, 37 °C). The cells were washed with PBS and incubated with fluorescent-labeled secondary antibodies (Alexa 488-labeled goat anti-mouse IgG) for 1 h at 37 °C. Afterward, the cells were counterstained with DAPI (5 min), thoroughly washed and analyzed by confocal microscopy (Nikon, A1 Multiphoton, Tokyo, Japan).

Immunofluorescent analysis with double staining was performed to confirm that the obtained contrast agent binds to the cells as an entire construction without any dissociation and/or cleavage. For this purpose glioma C6 cells were exposed to fluorescein-labeled mAb-PLL–DTPA-Gd and IgG-PLL–DTPA-Gd contrast agents (2 μM contrast agent, 45 min, 37 °C). Cells were washed with PBS, fixed with 4% paraformaldehyde and pre-incubated with 10% goat serum. Then cells were incubated with fluorescent-labeled secondary antibodies (Alexa 594-labeled goat anti-mouse IgG) for 1 h at 37 °C, washed with PBS and analyzed by fluorescent microscopy (DMI 6000, Leica, Wetzlar, Germany).

4.7. *In vivo* MRI analysis

All studies on animals were approved by the Ethical Committee of Pirogov Russian State Medical University and the experimental protocols followed were in accordance with institutional guidelines. Glioblastoma multiforme was modeled by stereotaxic injection of glioma C6 cells into the striatum region of rat brain (8 weeks female Wistar rats, n = 12) (36); see details in the Supporting Information. Two weeks after implantation of C6 cells the tumor growth and its location were verified by T_2-weighted MRI (Fig. 4(c)). When the tumor was approximately 14 ± 2% of the total area of the hemisphere section, animals were randomized based on tumor area into three groups (four rats per group). Then specific contrast agent mAbCx43-PLL–DTPA-Gd, nonspecific IgG-PLL–DTPA-Gd and Magnevist® were injected into the femoral vein at an equivalent dose of 0.05 mmol Gd/kg. MRI scanning was performed on a 7 T tomograph (ClinScan, Bruker BioSpin, Ettlingen, Germany) before and at 5 min and 1, 4, 6 and 24 h after injections. Tumor visualization was carried out in a turbo spin echo sequence with the following parameters: TR = 5000, TE = 57, resolution 320 × 288, slice thickness = 0.7 mm, FOV = 40 mm, turbo factor = 9. Contrast accumulation was investigated in the FLASH 2D regime with the following parameters: TR = 400, TE = 4, flip angle = 70°, resolution 256 × 256, slice thickness = 0.7 mm, FOV= 35 mm. The images of the body were acquired using a FLASH 2D sequence with fat suppression with the following parameters: TR = 409 ms, TE = 4.09 ms, flip angle = 70°, slice thickness = 1 mm, FOV = 50 × 42 mm, base resolution 384 × 324, number of acquisitions = 1.

4.8. MRI image analysis

Signal intensities of tumor and normal brain tissues were measured using syngo fastView (Siemens, Erlangen, Germany) and MultiVox Viewer (GammaMed, Moscow, Russia) software. Contrast enhancement of tumor tissue or contrast-to-noise ratio (CNR) for each time point was calculated according to the following equation (15): $CNR = (SI_{tumor} - SI_{normal})/SI_{noise}$, where SI_{tumor} is averaged signal intensities within the tumor, SI_{normal} is averaged signal intensities of normal tissue and SI_{noise} is averaged signal intensities of noise outside the rodent head (in the air).

The percent increase of CNR for each animal was calculated in comparison with pre-injection data: $\%CNR = (CNR_{post}/CNR_{pre}) \times 100\%$, where CNR_{pre} is the CNR value before injection and CNR_{post} the CNR value after injection of contrast agent at each time point.

Relative tumor area after injection of contrast agent was calculated based on region of interest measurement in the MRI image for equal segments of rat brain: $\Delta V_{tumor}\ (\%) = (V_{post} - V_{pre})/V_{pre}$, where V_{post} is the averaged area of visualized tumor tissue after injection of contrast agent and V_{pre} the averaged area of tumor tissue before injection.

4.9. *In vivo* accumulation of targeted contrast agents

Rats with intracranial glioma C6 received Alexa 647-labeled contrast agents (specific Cx43 and nonspecific IgG contrast agents, PLL–DTPA adduct) by i.v. injection at a dose of 2 mg of contrast agent/rat. After 24 h transcardial perfusion with 4% paraformaldehyde was performed, and major organs and brains were collected. The fluorescence measurements of the organs and brains were made on an IVIS Spectrum CT (Perkin Elmer, Waltham, MA, USA) with excitation/emission wavelength filters at 600, 640 nm/620, 640, 660 and 680 nm. The separation of signals from tissue and contrast agents was performed with Living Image 4.4 software (Perkin Elmer, Waltham, MA, USA). Fluorescent signals of the organs and brains were measured as average radiance (p/s/cm^2/sr). Brains were sliced using a cryostat (30 μm,

MNT SLEE cryostat, Mainz, Germany), stained with DAPI and analyzed using fluorescent microscopy (DMI 6000, Leica, Wetzlar, Germany).

4.10. Statistical analysis

Statistical analysis was performed using a Student *t*-test with the Microsoft Office Excel 2007 program. Differences were considered statistically significant when $p < 0.05$.

Acknowledgements

This work was supported by RFBR grant 13-04-01383, RSF grants 14-15-00698 (glioma modeling) and 14-13-00731 (MRI analysis), and Grant 11.G34.31.0004 of the Russian Federation Ministry of Science and Education. We thank Dr Vladimir Baklaushev and Pavel Melnikov for their help with confocal imaging.

REFERENCES

1. Brandes AA, Tosoni A, Franceschi E, Reni M, Gatta G, Vecht C. Glioblastoma in adults. Crit Rev Oncol Hematol 2008; 67(2): 139–152.
2. Siegel R, Ma J, Zou Z, Jemal A. Cancer statistics, 2014. CA Cancer J Clin 2014; 64(1): 9–29.
3. Caravan P. Strategies for increasing the sensitivity of gadolinium based MRI contrast agents. Chem Soc Rev 2006; 35(6): 512–523.
4. Hesselink JR, Press GA. MR contrast enhancement of intracranial lesions with Gd-DTPA. Radiol Clin North Am 1988; 26(4): 873–887.
5. Hesselink JR, Healy ME, Press GA, Brahme FJ. Benefits of Gd-DTPA for MR imaging of intracranial abnormalities. J Comput Assist Tomogr 1988; 12(2): 266–274.
6. Maeda H. The enhanced permeability and retention (EPR) effect in tumor vasculature: the key role of tumor-selective macromolecular drug targeting. Adv Enzyme Regul 2001; 41: 189–207.
7. Zhou Z, Lu ZR. Gadolinium-based contrast agents for magnetic resonance cancer imaging. Wiley Interdiscip Rev Nanomed Nanobiotechnol 2013; 5(1): 1–18.
8. Opsahl LR, Uzgiris EE, Vera DR. Tumor imaging with a macromolecular paramagnetic contrast agent: gadopentetate dimeglumine–polylysine. Acad Radiol 1995; 2(9): 762–767.
9. Kornguth S, Anderson M, Turski P, Sorenson J, Robins HI, Cohen J, Rappe A, Markley J. Glioblastoma multiforme: MR imaging at 1.5 and 9.4 T after injection of polylysine–DTPA-Gd in rats. Am J Neuroradiol 1990; 11(2): 313–318.
10. Qiu LH, Zhang JW, Li SP, Xie C, Yao ZW, Feng XY. Molecular imaging of angiogenesis to delineate the tumor margins in glioma rat model with endoglin-targeted paramagnetic liposomes using 3T MRI. J Magn Reson Imaging 2015; 41(4): 1056–1064.
11. Huang R, Han L, Li J, Liu S, Shao K, Kuang Y, Hu X, Wang X, Lei H, Jiang C. Chlorotoxin-modified macromolecular contrast agent for MRI tumor diagnosis. Biomaterials 2011; 32(22): 5177–5186.
12. Oliveira R, Christov C, Guillamo JS, de Bouard S, Palfi S, Venance L, Tardy M, Peschanski M. Contribution of gap junctional communication between tumor cells and astroglia to the invasion of the brain parenchyma by human glioblastomas. BMC Cell Biol 2005; 6(1): 7.
13. Nagasawa K, Chiba H, Fujita H, Kojima T, Saito T, Endo T, Sawada N. Possible involvement of gap junctions in the barrier function of tight junctions of brain and lung endothelial cells. J Cell Physiol 2006; 208(1): 123–132.
14. Kotini M, Mayor R. Connexins in migration during development and cancer. Dev Biol 2015; 401(1): 143–151.
15. Sin WC, Crespin S, Mesnil M. Opposing roles of connexin43 in glioma progression. Biochim Biophys Acta 2012; 1818(8): 2058–2067.
16. Baklaushev VP, Yusubalieva GM, Tsitrin EB, Gurina OI, Grinenko NP, Victorov IV, Chekhonin VP. Visualization of Connexin 43-positive cells of glioma and the periglioma zone by means of intravenously injected monoclonal antibodies. Drug Deliv 2011; 18(5): 331–337.
17. Veronese FM. Peptide and protein PEGylation: a review of problems and solutions. Biomaterials 2001; 22(5): 405–417.
18. Arnold LJ Jr, Dagan A, Gutheil J, Kaplan NO. Antineoplastic activity of poly(L-lysine) with some ascites tumor cells. Proc Natl Acad Sci U S A 1979; 76(7): 3246–3250.
19. Langer R. Drug delivery and targeting. Nature 1998; 392(Suppl 6679): 5–10.
20. Bogdanov AA, Lewin M, Weissleder R. Approaches and agents for imaging the vascular system. Adv Drug Deliv Rev 1999; 37(1–3): 279–293.
21. Haefliger JA, Nicod P, Meda P. Contribution of connexins to the function of the vascular wall. Cardiovasc Res 2004; 62(2): 345–356.
22. Chekhonin VP, Baklaushev VP, Yusubalieva GM, Belorusova AE, Gulyaev MV, Tsitrin EB, Grinenko NF, Gurina OI, Pirogov YA. Targeted delivery of liposomal nanocontainers to the peritumoral zone of glioma by means of monoclonal antibodies against GFAP and the extracellular loop of Cx43. Nanomedicine 2012; 8(1): 63–70.
23. Knopp MV, von Tengg-Kobligk H, Floemer F, Schoenberg SO. Contrast agents for MRA: future directions. J Magn Reson Imaging 1999; 10(3): 314–316.
24. Weinmann HJ, Brasch RC, Press WR, Wesbey GE. Characteristics of gadolinium–DTPA complex: a potential NMR contrast agent. Am J Roentgenol 1984; 142(3): 619–624.
25. Haley TJ, Raymond K, Komesu N, Upham HC. Toxicological and pharmacological effects of gadolinium and samarium chlorides. Br J Pharmacol Chemother 1961; 17: 526–532.
26. Ekholm S, Jonsson E, Sandvik L, Fagerlund M, Holtas S, Isberg B, Lindell D, Linden B, Sjoberg S, Thuomas KA, Tollesson PO. Tolerance and efficacy of Omniscan (gadodiamide injection) in MR imaging of the central nervous system. Acta Radiol 1996; 37(2): 223–228.
27. Tiutin LA, Panfilenko AF, Arzumanova NV, Fedotova IG, Berezin SM, Shelkoplias EN. Magnetic resonance tomography using the contrast preparation Magnevist. Vestn Rentgenol Radiol 1996; 2: 6–13.
28. Vexler VS, Clement O, Schmitt-Willich H, Brasch RC. Effect of varying the molecular weight of the MR contrast agent Gd-DTPA-polylysine on blood pharmacokinetics and enhancement patterns. J Magn Reson Imaging 1994; 4(3): 381–388.
29. Marchal G, Bosmans H, Van Hecke P, Speck U, Aerts P, Vanhoenacker P, Baert AL. MR angiography with gadopentetate dimeglumine–polylysine: evaluation in rabbits. Am J Roentgenol 1990; 155(2): 407–411.
30. Schuhmann-Giampieri G, Schmitt-Willich H, Frenzel T, Press WR, Weinmann HJ. In vivo and in vitro evaluation of Gd-DTPA-polylysine as a macromolecular contrast agent for magnetic resonance imaging. Invest Radiol 1991; 26(11): 969–974.
31. Caravan P. Protein-targeted gadolinium-based magnetic resonance imaging (MRI) contrast agents: design and mechanism of action. Acc Chem Res 2009; 42(7): 851–862.
32. Orth RC, Bankson J, Price R, Jackson EF. Comparison of single- and dual-tracer pharmacokinetic modeling of dynamic contrast-enhanced MRI data using low, medium, and high molecular weight contrast agents. Magn Reson Med 2007; 58(4): 705–716.
33. Singh R, Lillard JW Jr. Nanoparticle-based targeted drug delivery. Exp Mol Pathol 2009; 86(3): 215–223.
34. Han L, Li J, Huang S, Huang R, Liu S, Hu X, Yi P, Shan D, Wang X, Lei H, Jiang C. Peptide-conjugated polyamidoamine dendrimer as a nanoscale tumor-targeted T1 magnetic resonance imaging contrast agent. Biomaterials 2011; 32(11): 2989–2998.
35. Zhang D, Feng XY, Henning TD, Wen L, Lu WY, Pan H, Wu X, Zou LG. MR imaging of tumor angiogenesis using sterically stabilized Gd-DTPA liposomes targeted to CD105. Eur J Radiol 2009; 70(1): 180–189.
36. Chekhonin VP, Baklaushev VP, Yusubalieva GM, Pavlov KA, Ukhova OV, Gurina OI. Modeling and immunohistochemical analysis of C6 glioma *in vivo*. Bull Exp Biol Med 2007; 143(4): 501–509.
37. Baklaushev VP, Gurina OI, Yusubalieva GM, Dmitriev RI, Makarov AV, Chekhonin VP. Isolation of extracellular recombinant fragment of rat connexin-43. Bull Exp Biol Med 2009; 148(3): 389–393.
38. Tamura H, Yanagawa I, Hikichi T, Matsumoto K, Takahashi S, Sakamoto K. T1 measurements with clinical MR units. Tohoku J Exp Med 1995; 175(4): 249–267.

SUPPORTING INFORMATION

Additional supporting information may be found in the online version of this article at the publisher's web site.